PERGAMON

Vision Research 42 (2002) 1413–1420

Vision Research

www.elsevier.com/locate/visres

Spatial frequency tuning of the Ouchi illusion and its dependence on stimulus size

Hiroshi Ashida *

Graduate School of Letters, Kyoto University, Kyoto 606-8501, Japan

Received 3 January 2001; received in revised form 11 March 2002

Abstract

This study investigated the effects of the stimulus size on the spatial frequency tuning of the Ouchi illusion, which is an illusory sliding motion perceived in a checkerboard pattern of rectangular elements that is surrounded by a checkerboard pattern of orthogonally oriented elements. Two experiments were conducted to measure the perceived strength of illusion. The optimal size of the inner pattern increased proportionally with check size. In contrast, the optimal check size increased with the size of the inner pattern but not proportionally, and the range of increase was relatively small. The optimal fundamental spatial frequency was lower for a larger stimulus both for checkerboard patterns and simpler sinusoidal grating patterns, but there were differences in the tuning curves for the two types of stimuli. These results support the idea that two processes underlie the Ouchi illusion; one computes the local motion direction, and the other integrates motion signals across space for surface segmentation. For the checkerboard and grating stimuli, the former process may be different while the latter can be shared.

Keywords: Motion perception; Ouchi illusion; Spatial frequency

1. Introduction

When a rectangular checkerboard pattern is surrounded by an orthogonally oriented checkerboard pattern, the inner pattern appears to slide to and fro (Fig. 1a). Spillmann and Werner (1990) found this pattern [1] in a book of design collection by a Japanese designer Ouchi (1977). This book only contains figures without any words, and we cannot find who created this figure or if the author was aware of the illusion. Among many optical art figures, Ouchi may not have had particular interest in this figure. In the original figure, the checks in the outer area gradually become squares toward the outer edges, but this is not crucial for the illusion. A reduced pattern that consists of sinusoidal gratings has a similar effect (Fig. 1b), and has been used in experiments (Hine, Cook, & Rogers, 1995, 1997).

The Ouchi illusion is caused by retinal motion either by eye or image motion. Illusory relative motion was observed under retinal image stabilisation when the image was oscillated (Spillmann, Tulunay-Keesey, & Olson, 1993), though the apparent motion was perceived both in the inner and outer fields. The illusion therefore should reflect some cortical motion processing in our visual system.

It has been argued that this illusion arises in the process of integrating local motion signals (Fermüller, Pless, & Aloimonos, 2000; Hine et al., 1997; Mather, 2000). Given that the front-end motion detectors have one-dimensional spatial receptive fields (e.g. Adelson & Bergen, 1985; DeAngelis, Ohzawa, & Freeman, 1993; van Santen & Sperling, 1985) that suffer from an aperture problem, outputs of multiple detectors must be integrated into two-dimensional motion signals (e.g. Wilson, Ferrera, & Yo, 1992). If this integration process does not always give veridical outputs but produces biases towards the direction that is perpendicular to the longer edges of the checks, it will lead to an illusory relative motion between the two areas of the Ouchi figure. Fermüller et al. (2000) explained this directional bias based on statistical analyses; in the presence of noise, the estimation of motion direction with a general least-square method is biased depending on the reliabilities of motion signals. In short, motion signals along the longer edge are more reliable than those along the shorter edge, and the estimation is biased toward the

* Tel./fax: +81-75-753-2445.
E-mail address: ashida@bun.kyoto-u.ac.jp (H. Ashida).

[1] First reported by Spillmann, Heitger, and Schüller (1986).

0042-6989/02/$ - see front matter
PII: S0042-6989(02)00064-0

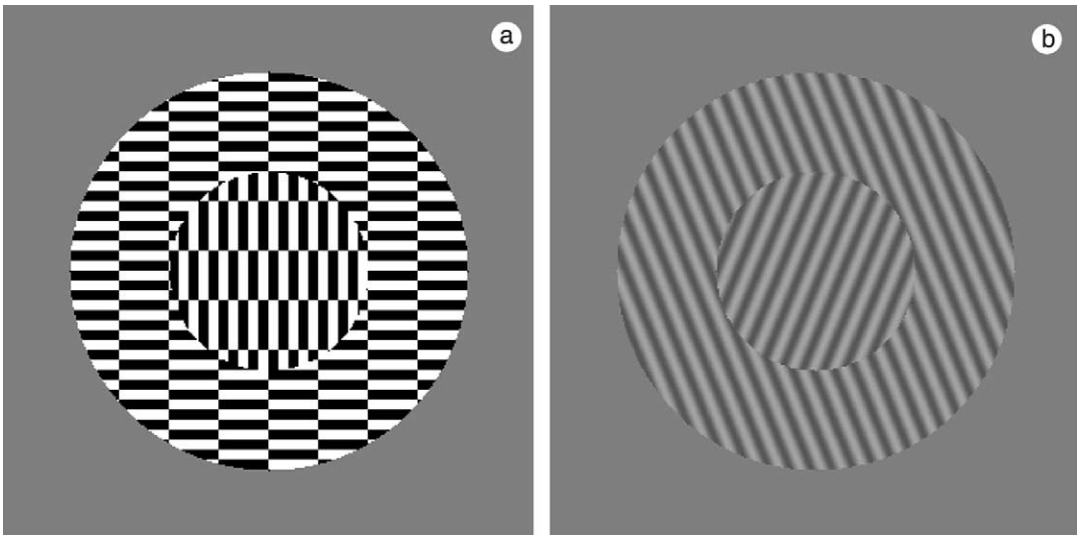

Fig. 1. Examples of the Ouchi pattern used in the experiments. The inner disk appears to float around. (a) The checkerboard pattern. The largest illusion is observed when the figure is moved back and forth in a diagonal direction. (b) The grating pattern that consists of sinusoidal gratings in different orientations. Good illusion is observed when the figure is moved up and down.

direction perpendicular to the longer edge. Mather (2000) also argued that this "orthogonal bias" produces the illusion in motion integration, suggesting a Bayesian framework to explain the bias.

A curious feature of this illusion is that it is tuned to fairly high spatial frequencies. Khang and Essock (1997a) reported that the optimal check size for this illusion is about 5×25 arcmin. A checkerboard pattern has fundamental Fourier components in two diagonal orientations, and the spatial frequency of the fundamental components is 6.1 c/deg in this case. Hine et al. (1995, 1997), using a reduced pattern that consisted of sinusoidal gratings, reported that the optimal spatial frequency is around 10 c/deg. Hine et al. (1997) pointed out that the tuning curve resembles that of the grating cells found in macaque V1 and V2 (von der Heydt, Peterhans, & Dursteler, 1992), and conjectured that these cells may be the source of the directional biases.

Fermüller et al. (2000) argued that high spatial frequency tuning is a result of the later stage of surface segmentation, as outlined below. This is an interesting idea, as the aspect of segmentation has not been much attended in studies of the Ouchi illusion. Actually, the Ouchi pattern induces a perception of two separate surfaces in different depths. The inner disk is seen either as floating or as a hole looking onto a distant wall. This sense of depth is considered to arise as a result of the illusory relative motion, although there may be an interaction that enhances the illusory motion in return. The idea of Fermüller et al. is that motion boundaries can be found by the residual error within a certain region, which can be calculated by a process that receives input from local detectors. Residual errors are small when the receptive fields of such a process fall within either inner or outer area, but they become large when the receptive fields cover both areas, because the motion signals are differently biased. Thus there will be a boundary between differently moving areas if the residual error is much larger than that in the neighbouring positions. Clear segmentation is possible when the receptive fields are relatively small as to the inner disk. When the receptive fields are relatively large, however, the boundaries would be blurred and the inner-disk may not be clearly segmented (see Fermüller et al., 2000, Fig. 11). Given that the receptive fields are generally larger for lower spatial frequencies, this smoothing effect would be larger for lower spatial frequencies, which accounts for the reduction of the Ouchi illusion for lower spatial frequencies.

Fermüller et al. (2000) presented computational analyses without showing experimental evidence for the effect of segmentation on the reduction of illusion at lower spatial frequencies. Here, a testable prediction is that the smoothing has less effect on the illusion for a larger inner disk, and therefore the optimal spatial frequency would be lower for a larger inner disk. However, no results are available on this matter. The inner disks used were of similar sizes: 1.65° in Khang and Essock (1997b), 1.0° in Khang and Essock (1997a), and 1.45° in Hine et al. (1995, 1997). One may argue that in all these cases the inner disk fell within the fovea, but it does not seem important because Mather (2000) used a mach larger pattern of 7.0° to report similar effects. In all these studies, the effect of the disk size was not directly assessed.

In this study, therefore, the effects of stimulus size on the optimal spatial frequency of the Ouchi illusion were examined in two experiments. In experiment 1, the effects of stimulus size and check size were investigated

using the checkerboard stimuli. In experiment 2, the checkerboard and the simplified grating stimuli (Hine et al., 1995, 1997) were compared as to the spatial frequency tuning. Generally larger stimuli yielded lower optimal spatial frequencies, which is compatible with the above prediction. The results will be discussed in terms of the possible role of the surface segmentation process, and the difference in the two types of stimuli.

2. Experiment 1

2.1. Method

2.1.1. Apparatus and stimuli

Stimuli were generated by a frame buffer system (Cambridge Research System, VSG 2/3) and presented on a SONY 21″ CRT. The screen refresh rate was 100 Hz, and the average luminance was 27 cd/m^2. Observers viewed the screen from a distance of 80 cm with the aid of a chin rest in a dim room. They responded through a numerical keypad attached to the computer.

The stimulus consisted of a circular patch of vertically oriented checks located in the centre of a larger circular patch of horizontally oriented checks (Fig. 1a). The size of the outer disk was always 16.0° in diameter, and the size of the inner disk was varied (0.9, 1.8, 3.5, 7.0, and 14.0° in diameter). The ratio of the long and the short sides of check elements was always 5:1. So the length of the longer side, which is referred to as the element length, is used to indicate the size of the elements throughout this paper. Five element lengths were tested for each inner-disk size (15, 23, 30, 45, and 60 min arc). The Michelson contrast of the checkerboard pattern was always 100%. The rest of the screen area was filled with average grey (27 cd/m^2). The spatial phases of the checkerboard patterns were randomised for each presentation.

2.1.2. Procedure

The strength of the illusory sliding motion was measured by rating as was used in previous studies (Hine et al., 1997; Khang & Essock, 1997a,b; Mather, 2000). Observers rated the strength of the perceived sliding motion of the inner pattern, relative to the outer pattern. They were instructed to give 0 only when there was no illusory motion at all, and give 1–4 according to the strength of the illusion. They were instructed to use the full scale, and completed at least two practice sessions to build up stable subjective response criteria.

Observers started each observation from the centre, by looking at the central fixation mark and pressing a key. The fixation mark was removed during the stimulus presentation. A stimulus pattern was presented for 4 s, remaining stationary on the screen. Observers were instructed to scan the entire stimulus area with eye movement. After each presentation, observers responded by pressing one of the number keys.

All 25 combinations of inner-disk size and element length were presented once in an experimental session in random order. Eight sessions were completed by each observer after practice.

2.1.3. Observers

Three naïve observers participated as part of their job assignment. All had normal or corrected-to-normal vision.

2.2. Results

Fig. 2 shows contour plots (using the software "DeltaGraph") of the results in which average ratings of illusion are plotted as a function of the element size and inner-disk size. For all three observers, the ridgeline lies in the diagonal orientation, which means that the optimal element size depends on the inner-disk size and the optimal inner-disk size depends on the element size. These two points have different implications beyond just two aspects of the same thing, as discussed in the next sections, because of rather different ranges of the two parameters.

Fig. 3a shows average ratings as a function of element length. Gaussian functions were fitted on a log scale (base = 10) to the data for each inner-disk size. The peak element lengths of the Gaussian curves were plotted as a function of inner-disk size in Fig. 3b. The optimal check

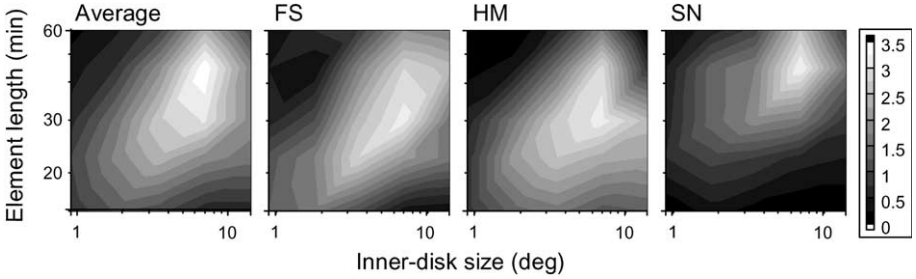

Fig. 2. Summary of the results in experiment 1 as contour plots. The rating scores are plotted as a function of the disk size and the element length for the average and the individual observers. A lighter area shows stronger illusion observed.

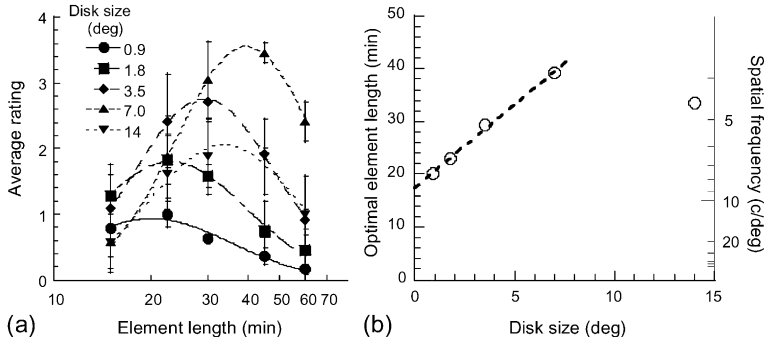

Fig. 3. (a) The results of experiment 1, re-plotted from Fig. 2 as a function of element length for each inner disk size. The curves show the fitted log-Gaussian functions. Error bars show standard errors of mean across observers. (b) Optimal element length derived from the fitted curves, as a function of inner-disk size. Corresponding fundamental spatial frequencies are shown on the right axis. The dotted line shows the fitted linear function for the first four points.

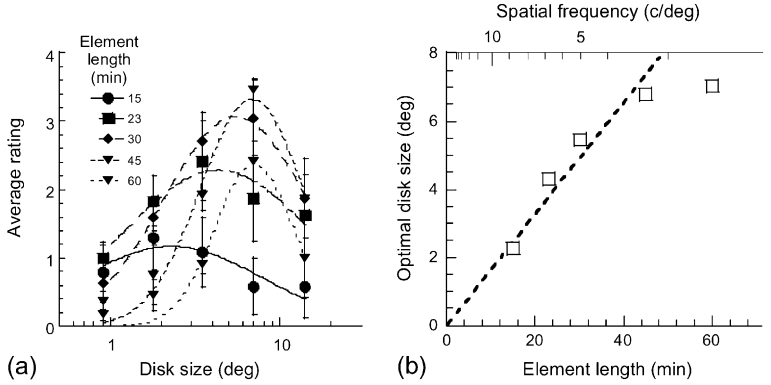

Fig. 4. (a) The results of experiment 1, re-plotted from Fig. 2 as a function of inner-disk size. The curves show the fitted log-Gaussian functions. Error bars indicate standard errors of mean. (b) Optimal inner-disk size derived from the fitted curves, as a function of element length. Corresponding fundamental spatial frequencies are shown on the top. The dotted line shows the fitted linear function for the first four points, assuming that the intercept is zero.

size increased linearly as the inner-disk size increased, except for the largest size. In other words, the optimal spatial frequency decreased as the inner disk became larger down to about 4 c/deg, as shown on the right ordinate. Complete scale invariance would have led to an intercept of zero, but the intercept of the fitted line (17.5 arcmin) was clearly above zero. When the inner-disk size increased from 0.9 to 7.0, by a factor of 7.8, the optimal element size increased from 20.0 to 39.2, only by a factor of 2.0.

Fig. 4a shows average ratings as a function of inner-disk size (replotted from Fig. 3a). Gaussian functions were fitted and the peak disk sizes were plotted as a function of element length in Fig. 4b. Optimal inner-disk size increased proportionally with element length, except for the largest length. The dashed line in the figure represents the fitted linear function with zero intercept for element lengths up to 45 arcmin. The fit is good ($r^2 = 0.92$), indicating scale invariance within this range.

The deviation of the data for the largest inner-disk size and the largest element length may indicate the absolute size limit of this illusion, but it may also reflect the outer disk whose diameter was constant. There must be an upper limit in the increase of the illusion at a certain disk size, but it is beyond the scope of this paper.

3. Experiment 2

The purpose of this experiment was to compare the effects of stimulus size on the optimal spatial frequency for patterns consisting of checks and sinusoids. The stimuli were oscillated on the screen along the optimal axis for each type of stimulus. Instead of using a constant outer disk, the ratio of inner and outer disks was set constant in this experiment.

3.1. Method

3.1.1. Apparatus and stimuli

Two types of stimuli were used in this experiment: (1) checkerboard patterns as in experiment 1, and (2) sinusoidal grating stimuli as used by Hine et al. (1995, 1997). To allow smooth diagonal oscillation, the check-

erboard stimuli were generated with a Windows-based PC using DirectDraw functions and displayed on a Hitachi 21″ CRT, with a refresh rate of 100 Hz and an average luminance of 59 cd/m^2. The ratio of long and short sides was 5:1, and the contrast was 100%. The grating stimuli were generated with VSG 2/3 and displayed on a SONY 21″ CRT with a refresh rate of 100 Hz and an average luminance of 64 cd/m^2. The grating in the inner disk was oriented 22° clockwise from the vertical and the grating in the outer disk was oriented 22° anticlockwise from the vertical, so that the angle between them was nearly the optimal value of 45° (Hine et al., 1995).

The contrast of the sinusoid stimuli was set to be 15 times the detection threshold. The detection threshold was measured by a method of adjustment for an inner disk of 8.0° diameter, without the outer area, that oscillated in the same way as in the main experiment. The threshold values of a trained observer were used to determine the stimulus contrast of the main experiment. The threshold values of naive observers were liable be higher but the relative thresholds across spatial frequencies were very similar to those of the trained observer.

The size of the inner disk was 1.5, 3.0, or 6.0° in diameter. The element length of the checkerboard stimuli was 15, 23, 30, 45, or 60 arcmin. The spatial frequency of the fundamental component was 10.2, 6.8, 5.1, 3.4, or 2.5 c/deg, respectively, and these five frequencies were used for the grating stimuli.

The checkerboard stimuli also oscillated sinusoidally at 1.9 Hz through a distance of 0.26° along the optimal axis of 45° clockwise from the vertical (Mather, 2000). The grating stimuli oscillated sinusoidally at 1.9 Hz through a distance of 0.26° along the vertical axis.

3.1.2. Procedure

A fixation mark appeared in the centre and the observer initiated a trial by pressing a key. Then, a stimulus was presented for four cycles (2.0 s), and observers rated the strength of illusion. As in experiment 1, they gave 0 for no illusion and gave 1–4 for any perceived illusion. The fixation mark was absent during the stimulus presentation so it would not interfere with illusory motion of the inner disk. Thus observers were not required to maintain strict fixation, but they were instructed to maintain their gaze roughly at the centre without scanning the figure. In addition, the observation time was halved relative to that used in experiment 1, to reduce the possibility of free scanning.

All 15 combinations of stimuli were presented once in a session in random order. After at least two sessions of practice, each observer completed six experimental sessions.

3.1.3. Observers

Eight naïve observers participated, either as part of their job assignment, or as paid volunteers. All had normal or corrected-to-normal vision. Two participated in both the checkerboard and the grating tests. Three participated only in the checkerboard test, and the other three participated only in the grating test. So each test was completed by five observers.

3.2. Results

Fig. 5 plots the averaged ratings from all five observers for both checkerboard stimuli (a) and grating stimuli (b), as a function of the fundamental spatial frequency. For both checkerboard and grating stimuli, the peaks lie in a relatively high spatial frequency range. As in experiment 1 (Fig. 3), the peaks shifted towards lower spatial frequency as the inner disk became larger. For the checkerboard stimuli (Fig. 5a), Gaussian functions were fitted to the data on a log scale for each inner-disk size. For the grating stimuli (Fig. 5b), however, the data were not symmetrical and Gaussian functions failed to give a good fit on a log scale, but gave a fairly good fit on a linear scale. This is because the fall-off at

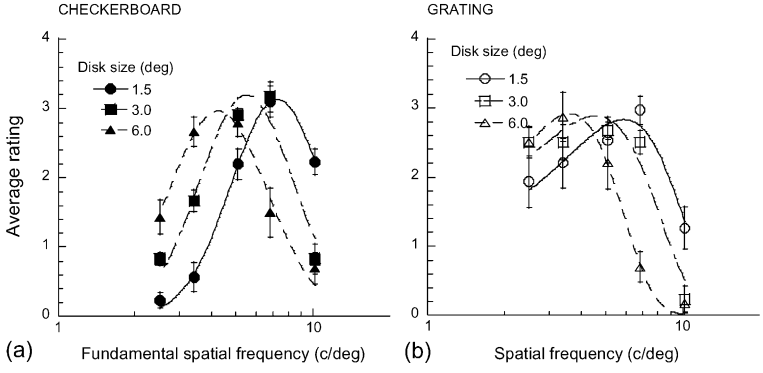

Fig. 5. The results of experiment 2. Average ratings are plotted as a function of the spatial frequency for each inner-disk size. (a) The results for the checkerboard stimuli. Curves show fitted Gaussian functions on the log scale. (b) The results for the grating stimuli. Curves show fitted Gaussian functions on the linear scale. In both figures, error bars show standard errors of mean across observers.

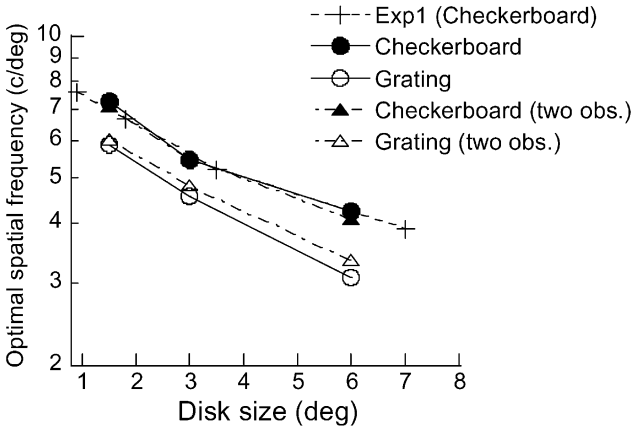

Fig. 6. The optimal spatial frequencies for checkerboard and grating stimuli in experiment 2, derived from the fitted curves in Fig. 5. Circles show the results from all the observers. Crosses show the results of experiment 1, re-plotted from Fig. 3b. Triangles show the results of the two observers who were tested with both checkerboard and grating stimuli. Filled symbols are for checkerboard stimuli, and open symbols are for grating stimuli.

the low spatial frequency end was relatively small for sinusoidal stimuli.

Fig. 6 plots log optimal spatial frequency as a function of inner-disk size, calculated from the averages of the five observers, for closer look at the shift of optimal spatial frequencies. Data from experiment 1 (+) are shown as well. The results for checkerboard stimuli in experiments 1 and 2 largely overlap, indicating the accuracy of the derived optimal frequencies regardless of the differences in the size of the outer disk (constant in experiment 1 and proportional in experiment 2) and in the mode of presentation (stationary in experiment 1 and oscillating in experiment 2). The optimal spatial frequency decreased with increasing inner-disk size. The results for the grating stimuli showed a similar decrease with inner-disk size, but the absolute frequencies were systematically lower by a factor of 0.7–0.8. This difference is not due to the difference between observers, because the results of the two observers who participated in both the checkerboard and the grating experiments showed a similar tendency (as indicated by filled and open triangles).

4. General discussion

4.1. Evidence for a segmentation process

The results support the idea that a later segmentation process is involved in the Ouchi illusion (Fermüller et al., 2000). The optimal inner-disk size increased proportionally with the inverse of the spatial frequency (Fig. 4). This result can be explained by assuming that the segmentation process has larger receptive fields for lower spatial frequencies. Thus, to be clearly segmented a larger area is needed at lower spatial frequency.

Similarly, the optimal spatial frequency decreased (i.e., the optimal check size increased) as the inner-disk size increased both for checkerboard and grating stimuli (Figs. 3 and 6). In other words, lower spatial frequency is preferred for a larger inner disk. In this case, however, the optimal spatial frequency varied in a relatively small range, suggesting that the segmentation process is not the sole cause of the reduction of the illusion at lower spatial frequencies.

The role of surface segmentation process is also suggested by a recent demonstration that a pattern that does not comprise any directional bias can yield a similar illusion. Spillmann and Pinna (2000) created an array of circular dots that are black in the central region and white in the surrounding region, thereby producing an illusory perception of floating motion. This illusion cannot be explained by the spatial structure alone but maybe by the difference in the speed signals for different polarity or contrast (Thompson, 1982). Another example is the jitter aftereffect (Murakami & Cavanagh, 1998), in which adaptation to a dynamic random noise yields an illusory jittering motion of the non-adapted region. This is also considered a segmentation based on differences in velocity (or temporal frequency) signals.

4.2. Spatial frequency tuning of the directional bias in checkerboard patterns

The results also suggest that the spatial frequency tuning of the process that produces local directional bias is band-pass shaped. The optimal frequency did not fall below 4 c/deg for checkerboard stimuli, which is still high for a motion phenomenon. The reduction of local bias itself for large check size can be explained based on statistical reliability of velocity estimates (Fermüller et al., 2000; Mather, 2000) if the reliability of signals along the shorter edges increase when it becomes longer while the reliability of signals along the longer edges may reach an asymptote. It is therefore expected that the Ouchi illusion reach the maximum at a medium spatial frequency irrespective of the tuning curve of the motion detection mechanism.

It is also possible that the perceived direction is corrected using second-order motion signals. The fundamental Fourier components of a checkerboard pattern comprises a plaid, which is a two-dimensional pattern made by adding two sinusoidal gratings in different orientations. It has been discussed that a second-order mechanism sensitive to the contrast modulation is partially responsible to the percept of plaid motion direction (Derrington & Badcock, 1992; Wilson, 1994). It is also suggested that the second-order system works as a feature tracking of the blobs in a plaid pattern (Derrington & Ukkonen, 1999). If so, large and easily disc-

ernable blobs would favour feature tracking, giving the veridical direction more effectively at relatively low spatial frequencies.

4.3. Difference in checkerboard and grating patterns

Note that the discussion in the previous section only applies to checkerboard patterns. In experiment 2, it was found that the spatial frequency tuning of the sliding illusion for grating patterns was systematically lower than that for checkerboard patterns. The reduction of illusion for lower spatial frequencies was smaller and the optimal spatial frequencies were lower. It is conceivable that the spatial frequency tuning of the local motion estimation process may be different for the grating and the checkerboard patterns. In the case of grating patterns, only the velocity normal to the orientation of the grating can be estimated in the middle of the pattern (aperture problem). The veridical direction is given at the edges when the disk itself moves, but signals at the edges may be too weak to correct the overall bias. In the case of the checkerboard pattern, in contrast, there is no such ambiguity. The different tuning functions especially at lower spatial frequencies may be a signature of different operations or mechanisms for these two types of stimuli. Moreover, as discussed above, the perceived direction may be affected by the second-order information with the checkerboard pattern, which cannot happen with the grating stimuli.

4.4. The Ouchi pattern as a plaid

Although it is out of the range of what the present data can tell, I would point out that the Ouchi illusion may be understood by the known properties of plaid motion perception. A plaid pattern consists of two sinusoidal gratings in different orientations, and they are classified into types I and II by the perceived pattern direction relative to the two component directions (Ferrera & Wilson, 1987). In a type I plaid, the pattern direction lies in the middle of the two component directions, while in a type II plaid the pattern direction lies outside the two component directions. Ferrera and Wilson (1990) reported that the perceived direction of a type I plaid is not significantly biased, but that of a type II plaid is biased towards the component direction.

Fig. 7 illustrates the case when the pattern oscillated along the 45°orientation, which is reported optimal for the illusion (Mather, 2000). The lines (a, b, c, d) represent the fundamental components. The direction of each component is ambiguous because the motion vector can terminate wherever on the constraint line (dotted lines). A single grating within a circular aperture is then perceived in the normal vector direction (a–d in bold characters). Note that when the pattern moves in this

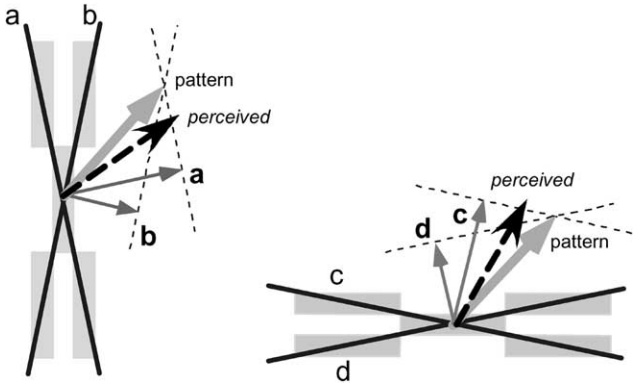

Fig. 7. Illustration of the moving checkerboard stimuli as type II plaids. Solid and dotted lines represent the fundamental components and their constraint lines of motion. The thick light arrows represent the pattern motion, and the thin arrows represent the component normal vectors. The perceived directions (thick dashed arrows) are biased towards their component vectors. The biases arise in the different directions in the two patterns, resulting in a relative motion between the two areas. See text for more details.

direction, both normal vectors (thin arrows) lie in one side of the pattern vector (thick light arrows). Thus both inner and outer patterns form type II plaid in this case, leading to biases toward the pattern direction (dashed arrows). As the biases are produced toward the opposite side of the pattern vector in the inner and the outer areas, relative motion between these two areas is maximised around this axis of oscillation. Oscillation along the vertical or horizontal direction produces little illusion, because the components form type I plaids in both areas. Robustness of the illusion is thus related to the range of pattern direction that yields type II plaids, which is determined by the aspect ratio of the checker elements.

Fermüller et al. (2000) described that their scheme can account for the biased direction perception in the type II plaid. Although they did not explain the direct relationship, it seems that this bias in the plaid motion perception would give a basis of explaining the Ouchi illusion in the spatiotemporal frequency space rather than in the image space based on the edges. A remaining problem is the fact that the illusion is stronger for a checkerboard pattern than for the component plaid pattern (Khang & Essock, 1997b). One may speculate that similar biases arise for harmonic components and then clearer segmentation is possible as a result of interaction across different spatial frequencies (Yo & Wilson, 1992).

As a concluding remark, this paper emphasises the merit of analysing the Ouchi illusion in the Fourier frequency space. Further theoretical works on the Ouchi illusion in relation to the literature on the Fourier analysis of our motion perception will in turn contribute to further understanding of our mechanism of visual motion perception.

Acknowledgements

I thank the anonymous reviewer for helpful comments and corrections. Experiments were conducted in Ritsumeikan University and ATR Human Information Processing Research Laboratories when the author was an employee. Portions of results were presented at International Congress of Psychology 2000 (Stockholm, Sweden) and European Conference on Visual Perception 2000 (Groningen, The Netherlands). Supported by JSPS Grant-in-aid for scientific research (A12710046).

References

Adelson, E. H., & Bergen, J. R. (1985). Spatiotemporal energy models for the perception of motion. *Journal of the Optical Society of America A, 2*, 284–299.

DeAngelis, G. C., Ohzawa, I., & Freeman, R. D. (1993). Spatiotemporal organization of simple-cell receptive fields in the cat's striate cortex. I. General characteristics and postnatal development. *Journal of Neurophysiology, 69*, 1091–1117.

Derrington, A. M., & Badcock, D. R. (1992). Two-stage analysis of the motion of 2-dimensional patterns: What is the first stage? *Vision Research, 32*(4), 691–698.

Derrington, A. M., & Ukkonen, O. I. (1999). Second-order motion discrimination by feature-tracking. *Vision Research, 39*, 1465–1475.

Fermüller, C., Pless, R., & Aloimonos, Y. (2000). The Ouchi illusion as an artifact of biased flow estimation. *Vision Research, 40*, 77–96.

Ferrera, V. P., & Wilson, H. R. (1987). Direction specific masking and the analysis of motion in two dimensions. *Vision Research, 27*, 1783–1796.

Ferrera, V. P., & Wilson, H. R. (1990). Perceived direction of moving two-dimensional patterns. *Vision Research, 30*, 272–287.

Hine, T. J., Cook, M., & Rogers, G. T. (1995). An illusion of relative motion dependent upon spatial frequency and orientation. *Vision Research, 35*, 3093–3102.

Hine, T. J., Cook, M., & Rogers, G. T. (1997). The Ouchi illusion: an anomaly in the perception of rigid motion for limited spatial frequencies and angles. *Perception and Psychophysics, 59*, 448–455.

Khang, B. G., & Essock, E. A. (1997a). Apparent relative motion from a checkerboard surround. *Perception, 26*, 831–846.

Khang, B. G., & Essock, E. A. (1997b). A motion illusion from two-dimensional periodic patterns. *Perception, 26*, 585–597.

Mather, G. (2000). Integration biases in the Ouchi and other visual illusions. *Perception, 29*, 721–727.

Murakami, I., & Cavanagh, P. (1998). A jitter after-effect reveals motion-based stabilization of vision. *Nature, 395*, 798–801.

Ouchi, H. (1977). *Japanese Optical and Geometrical Art*. New York: Dover.

Spillmann, L., Heitger, F., & Schüller, S. (1986). Apparent displacement and phase unlocking in checkerboard patterns. Poster presented at 9th European Conference on Visual Perception, Bad Nauheim (submitted late).

Spillmann, L., Tulunay-Keesey, Ü., & Olson, J. (1993). Apparent floating motion in normal and stabilized vision. *Investigative Ophthalmology and Visual Science, 34*(Suppl.), 1031.

Spillmann, L., & Pinna, B. (2000). An illusion of relative motion dependent upon figure-ground segregation. *Perception, 29*(Supplement), 112–113.

Spillmann, L., & Werner, J. S. (Eds.). (1990). *Visual perception: The neurophisiological foundations*. San Diego: Academic Press.

Thompson, P. G. (1982). Perceived rate of movement depends on contrast. *Vision Research, 22*, 377–380.

van Santen, J. P. H., & Sperling, G. (1985). Elaborate Reichardt detectors. *Journal of the Optical Society of America A, 2*, 300–321.

von der Heydt, R., Peterhans, E., & Dursteler, M. R. (1992). Periodic-pattern-selective cells in monkey visual cortex. *Journal of Neuroscience, 12*, 1416–1434.

Wilson, H. R. (1994). The role of second-order motion signals in coherence and transparency. In G. R. Bock, J. A. Goode, & C. Foundation (Eds.), *Higher-order processing in the visual system* (pp. 227–244). Chichester: John Wiley & Sons.

Wilson, H. R., Ferrera, V. P., & Yo, C. (1992). A psychophysically motivated model for two-dimensional motion perception. *Visual Neuroscience, 9*, 79–97.

Yo, C., & Wilson, H. R. (1992). Moving two-dimensional patterns can capture the perceived directions of lower or higher spatial frequency gratings. *Vision Research, 32*, 1263–1269.